

# RSC Advances



This is an *Accepted Manuscript*, which has been through the Royal Society of Chemistry peer review process and has been accepted for publication.

*Accepted Manuscripts* are published online shortly after acceptance, before technical editing, formatting and proof reading. Using this free service, authors can make their results available to the community, in citable form, before we publish the edited article. This *Accepted Manuscript* will be replaced by the edited, formatted and paginated article as soon as this is available.

You can find more information about *Accepted Manuscripts* in the [Information for Authors](#).

Please note that technical editing may introduce minor changes to the text and/or graphics, which may alter content. The journal's standard [Terms & Conditions](#) and the [Ethical guidelines](#) still apply. In no event shall the Royal Society of Chemistry be held responsible for any errors or omissions in this *Accepted Manuscript* or any consequences arising from the use of any information it contains.



## ARTICLE

## Navigating in chromone chemical space: discovery of novel and distinct A<sub>3</sub> adenosine receptor ligands.

F. Cagide,<sup>a</sup> A. Gaspar,<sup>a</sup> J. Reis,<sup>a</sup> D. Chavarria,<sup>a</sup> S. Vilar,<sup>b,c,\*</sup> G. Hripcsak,<sup>c</sup> E. Uriarte,<sup>b</sup> S. Kachler,<sup>d</sup> K. Klotz,<sup>d</sup> F. Borges<sup>a,\*</sup>

Received 00th January 20xx,  
Accepted 00th January 20xx

DOI: 10.1039/x0xx00000x

www.rsc.org/

One of the major hurdles in the development of safe and effective drugs targeting G-protein coupled receptors (GPCRs) is finding ligands that are highly selective for a specific receptor subtype. The search for novel compounds with therapeutic value by targeting the A<sub>3</sub> adenosine receptor (A<sub>3</sub>AR) is still in its early stages. The increasing knowledge about the biological, physiological and pathological role of A<sub>3</sub>AR subtype was escorted by the design and development of the A<sub>3</sub>AR ligands, but the particular role of A<sub>3</sub>AR agonists and antagonists is still an open issue.

Among the large variety of chemical classes screened towards ARs flavonoids have been indicated as remarkable A<sub>3</sub>AR antagonists. However, the search of A<sub>3</sub>AR ligands based on this framework seems to be discontinued. In this context, our research group focused its investigation into the discovery and development of novel, potent and selective ARs ligands based on the chemical core of flavonoids, the chromone scaffold. The ongoing research has shown that chromone-2-phenylcarboxamide derivatives display a remarkable tendency for A<sub>3</sub>AR. In this work we report stimulating results, supported by A<sub>2A</sub>/A<sub>3</sub> molecular docking simulations and structure-affinity-relationship (SAR) studies by which *N*-(4,5-methylthiazol-2-yl)-4-oxo-4*H*-chromene-2-carboxamide (compound **31**) emerged as the most potent and selective compound, displaying an *h*A<sub>3</sub> K<sub>i</sub> of 167 nM and a selectivity ratio of 590 vs. the A<sub>1</sub> and 480 vs. the *h*A<sub>2A</sub>AR subtypes. The chromone-based ligand was obtained by a simple synthetic approach and will enter in a lead optimization program to enhance its potency and drug-like properties.

### Introduction

Adenosine is a biomolecule that plays a well-known biological role as nucleic acid building block and as a component of the cellular ATP energy system. Outside of the cell, adenosine can act as a signalling molecule by interacting with four distinct adenosine receptors (ARs) — designated as A<sub>1</sub>, A<sub>2A</sub>, A<sub>2B</sub> and A<sub>3</sub>.<sup>1,2</sup> The ARs are G protein-coupled receptors (GPCRs) that modulate adenylate cyclase activity. A<sub>1</sub> and A<sub>3</sub> receptor subtypes couple preferentially to G<sub>i</sub> protein and thereby inhibit adenylyl cyclase leading to a reduced production of cyclic AMP (cAMP) while A<sub>2A</sub> and A<sub>2B</sub> subtypes stimulate the production of cAMP by coupling to G<sub>s</sub> proteins.<sup>3</sup> The extensive research dedicated to the physiological and pathological role of

extracellular adenosine allowed the connection between the cellular signals promoted by ARs and several types of pathologies, namely neurological, cardiovascular, inflammatory diseases and cancer.<sup>2,4</sup> Nowadays, all four adenosine receptors are recognized as valid targets for drug discovery and development programs.<sup>5</sup> Adenosine plays a crucial role in the cell progression pathway, either during apoptosis or during cytostatic state. It has been postulated that high levels of extracellular adenosine can have a profound impact on the growth of tumour masses.<sup>6</sup> Several lines of evidence show that ARs are potential drug targets for cancer treatment, but it seems that the A<sub>2A</sub> and A<sub>3</sub> subtypes are the most promising candidates.<sup>7</sup> In fact, human A<sub>3</sub>AR are overexpressed in tumor cells including leukemia, lymphoma, astrocytoma and melanoma tumor cells, and are in turn considered as a target for cancer therapy.<sup>8</sup> The receptor is also overexpressed in inflammatory cells being a putative target for the treatment of inflammatory disorders, such as rheumatoid arthritis (RA).<sup>8,9</sup> Moreover, A<sub>3</sub>AR mediated neuroprotective effects have been demonstrated although further studies are still needed.<sup>8,9</sup>

<sup>a</sup> CIQUP/Departamento de Química e Bioquímica, Faculdade de Ciências, Universidade do Porto, 4169-007 Porto, Portugal.

<sup>b</sup> Departamento de Química Orgânica, Facultad de Farmacia, Universidad de Santiago de Compostela, 15782 Santiago de Compostela, Spain.

<sup>c</sup> Department of Biomedical Informatics, Columbia University Medical Center, 10032 New York, USA.

<sup>d</sup> Institut für Pharmakologie und Toxikologie, Universität Würzburg, 97078 Würzburg, Germany

\*Corresponding Authors: Fernanda Borges, CIQUP/Department of Chemistry and Biochemistry, Faculty of Sciences, University of Porto, Porto 4169-007, Portugal. E-mail: [fborges@fc.up.pt](mailto:fborges@fc.up.pt); Santiago Vilar Department of Biomedical Informatics, Columbia University Medical Center, 10032 New York, USA. [qosanti@yahoo.es](mailto:qosanti@yahoo.es)

The increasing knowledge about the physiological and pathological role of A<sub>3</sub>AR subtype was escorted by the design and development of A<sub>3</sub>AR ligands. From these research projects, many chemical structures successfully emerged as potent A<sub>3</sub>AR agonists (Figure 1)<sup>8, 10-12</sup> and antagonists (Figure 2).<sup>8,10</sup> Paradoxically, both agonists and antagonists showed encouraging results namely in anticancer therapy.<sup>13-19</sup>

However, despite the intensive efforts in medicinal chemistry to design and synthesize selective A<sub>3</sub>AR agonists and antagonists (Figures 2 and 3) from a diversity of chemical classes few of them have reached the clinical phase.<sup>8</sup> Central drawbacks found for the lack of success include side effects, which are related to the ubiquity of the receptors, low absorption, short half-life and toxicity.<sup>8</sup>

Although benzopyran is considered a privileged structure, few studies were addressed towards its application in the discovery of new ARs ligands. In this context, coumarin (2H-chromen-2-one)<sup>20, 21</sup> and flavonoid (2-phenyl-4H-chromen-4-one)<sup>22-24</sup> cores were reported as motivating scaffolds. The chemical optimization of A<sub>3</sub>ARs ligands based on a flavonoid scaffold was reported by Karton *et al*<sup>23</sup> in a study that resulted in two selective A<sub>3</sub>AR ligands, **MRS 1088** and **MRS 1067** with K<sub>i</sub> values of 741 nM and 561 nM, respectively (Figure 3). Yet, albeit interesting data has been acquired the compounds' low aqueous solubility, among other explanations, may be one of the major problems that hampered progress of the drug discovery project. To the best of our knowledge, the search for new and more potent A<sub>3</sub>AR ligands based on the flavonoid core was discontinued.

Chromones are a group of naturally occurring compounds that are ubiquitous in nature.<sup>25</sup> Chemically they are oxygen-containing heterocyclic compounds with a benzoannulated γ-pyrone ring (benzo-γ-pyrone [(4H)-1-benzopyran-4-one]) having a great potential for chemical decoration allied with a broad spectrum of pharmacological activities.<sup>25</sup> These

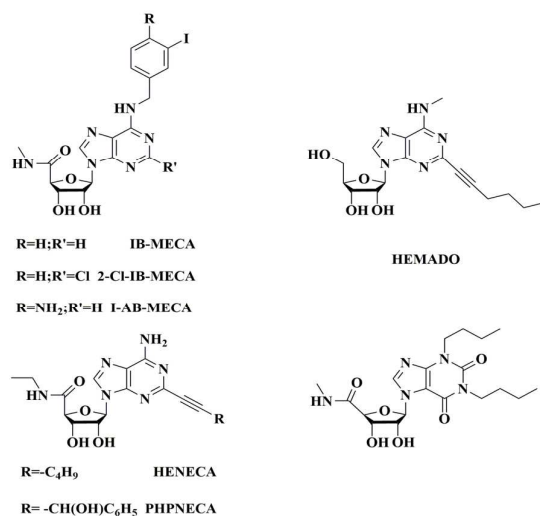


Figure 1. Examples of A<sub>3</sub>AR agonists based on adenosine and xanthine scaffolds

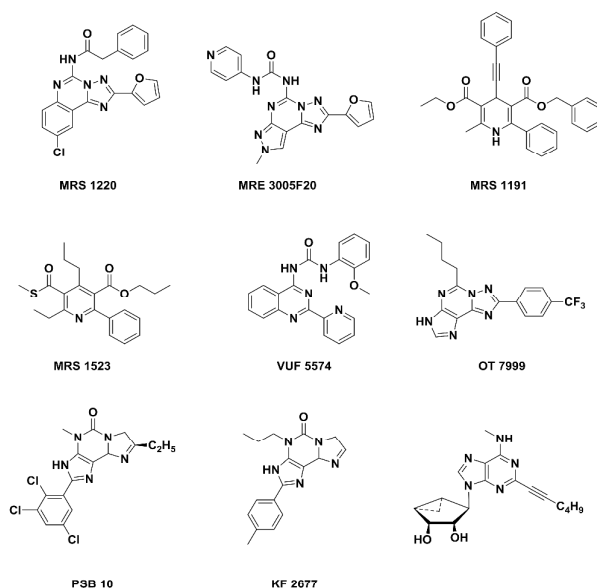


Figure 2. Examples A<sub>3</sub>AR antagonists based on triazoloquinazoline, dihydropyridine, pyrimidine, quinazoline, xanthine and adenosine scaffolds

features, along with the structural resemblance with flavonoids, inspired our group to initiate a medicinal chemistry program based on the chromone core in order to study its importance in the development of novel AR ligands.<sup>26, 27</sup> Preceding research performed by our group has shown that chromone-2-phenylcarboxamide is a valid scaffold for the design of novel A<sub>3</sub>AR ligands. Therefore, the present study was accomplished to acquire new data to validate the significance of the chromone-2-phenylcarboxamide framework. The study was guided by structure–affinity–relationships (SAR) performed with a new library of chromone compounds and complemented by molecular modeling studies.

## Results and discussion

### Chemistry

The novel chromone phenylcarboxamides were attained following synthetic strategies (Scheme 1) that encompassed a

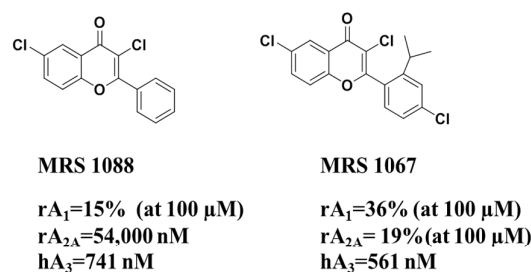


Figure 3. A<sub>3</sub>AR antagonists based on flavonoid scaffold.

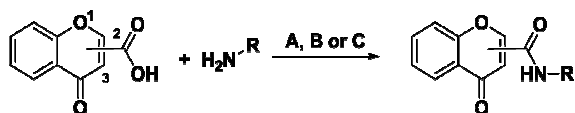
one-pot condensation between a chromone carboxylic acid and aryl or heteroaryl amine. The desired compounds were obtained in moderate to high yields. Strategy 1-A involved the activation of chromone-2-carboxylic (**1**) or chromone-3-carboxylic (**2**) acids by (benzotriazol-1-yloxy)tripyrrolidinophosphonium hexafluorophosphate (PyBOP) in the presence of *N,N*-diisopropylethylamine (DIPEA). After the subsequent addition of the suitable amine compounds **5-12**, **15-18**, **21-22**, **26-31** and **35** (Tables 1 and 2) were attained. Some chromone-2-carboxamides (**19**, **20**, **23**, **25**, **32**, Table 1) were obtained taking advantage of a microwave-assisted chemistry strategy 1-B. Briefly, the chromone-2-carboxylic acid (**1**) was activated by reaction with phosphorus oxychloride ( $\text{POCl}_3$ ) with formation of the corresponding acyl chloride, followed by a microwave-assisted amidation reaction that occurs between the obtained acyl chloride and the corresponding amine.<sup>28, 29</sup> Additionally, chromone-3-carboxamides **33** and **34** (table 2) were synthesised by a slightly modification of strategy 1-B due to the lability of the starting material and the inherent formation of enamine by-products.<sup>30</sup> The reaction of chromone-3-carboxylic acid (**2**) with  $\text{POCl}_3$  led to the formation of the corresponding acyl chloride and the amidation reaction took place at room temperature, without the employment of microwave heating (Scheme 1-C).

### Pharmacology

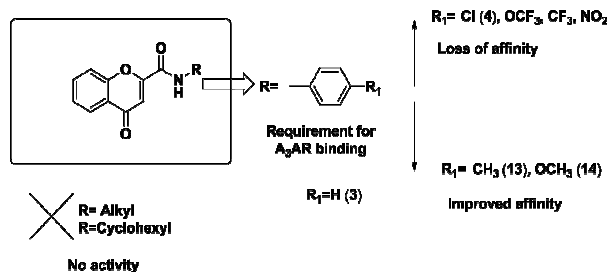
The affinity of the new potential antagonists for the human adenosine receptor subtypes  $hA_1$ ,  $hA_{2A}$ ,  $hA_3$  (expressed in Chinese hamster ovary (CHO) cells) was determined in radioligand competition experiments.<sup>11, 31-34</sup> In this assay, the competition with the following agonist radioligands: (i) [ $^3\text{H}$ ]CCPA at  $hA_1$  receptors, (ii) [ $^3\text{H}$ ]NECA at  $hA_{2A}$  and [ $^3\text{H}$ ]HEMADO at  $hA_3$  receptors was measured. The data were expressed as  $K_i$  (dissociation constant). The receptor binding affinities of the synthesised compounds (**3-35**) are reported in Tables 1 and 2.

### Structure-affinity relationship studies

Foregoing research of our group allowed acquiring evidence that validate chromone as a privileged structure for the design of adenosine receptor ligands and chromone-2-phenylcarboxamide (Scheme 2) as a new lead compound for the development of  $A_3$ AR ligands.<sup>26,27</sup> The structure-activity relationship (SAR) studies performed so far revealed the



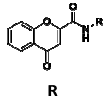







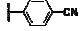













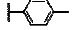





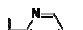


Scheme 1. Synthesis of chromone carboxamides. A-PyBOP, DIPEA, DMF,  $\text{CH}_2\text{Cl}_2$ , 0 °C to rt.; B-  $\text{POCl}_3$ , DMF, 120 °C, MW; C-  $\text{POCl}_3$ , DMF, rt.



Scheme 2. Preliminary structure-affinity relationships for chromone-2-carboxamide derivatives as  $A_3$ AR ligands (see also Table 1).<sup>26</sup>

importance of the phenylcarboxamide moiety as a key feature for receptor binding. Moreover, the location of the amide function at C-2 or C-3 position of the benzopyran nucleus and the type of amide, preferentially of aromatic type (**3**, Scheme 2, Table 1), has been found to modulate the affinity/selectivity of the compounds.<sup>26-27</sup> It has been also postulated that the presence of electron withdrawing (Scheme 2, Table 1) or donating groups (Scheme 2, Table 1) on the aromatic exocyclic ring seems to modulate the affinity and selectivity of chromone-2-phenylcarboxamide towards ARs subtypes.<sup>26-27</sup> New derivatives with carefully chosen substituents were synthesised in order to acquire more information about the significance of chromone-2-phenylcarboxamide as putative  $A_3$ AR ligand (Scheme 1, Table 1). Their influence on affinity and selectivity for human  $A_1$ ,  $A_{2A}$  and  $A_3$  ARs was evaluated in radioligand binding while the interaction with the  $A_{2B}$  AR was analyzed by adenylyl cyclase activity measurement following the procedures previously described by Klotz *et al.* with minor modifications.<sup>11, 31-34</sup> For all the tested compounds no measurable activity for  $A_{2B}$  AR ( $K_i > 10,000$  or 30,000 nM) was detected and therefore these values were omitted in Table 1. Previously, it was postulated that the presence of electron donors or withdrawing groups on the exocyclic aromatic system can modulate the affinity and selectivity of chromones.<sup>26</sup> Therefore, it was decided to synthesise a new chromone-2-phenylcarboxamide series that incorporates diverse types of substituents located at different positions of the exocyclic aromatic nucleus. These structural modifications, namely in *para* position, enabled the development of an extended SAR study. In accordance with the previous data, it was found that the introduction of different electron withdrawing substituents with dissimilar relative strengths from weak (-F, -Br, -I, compounds **5-7**), to moderate (- $\text{COCH}_3$ , - $\text{COOC}_2\text{H}_5$ , compounds **8** and **9**) and strong (-CN, compound **10**) results in all cases in compounds with no measurable affinity for all AR subtypes. Furthermore, a lack of affinity is also observed for a Cl-substituent in *para* (compound **4**), *ortho* (compound **11**) and *meta* (compound **12**) position of the exocyclic phenyl ring. Thus, the binding of chromone-2-phenylcarboxamides to AR is strongly influenced by electronic properties of the substituents and that any type of electron withdrawing groups located at any position of the exocyclic aromatic substituent is not tolerated.

Table 1. Affinity ( $K_i$ , nM; 95% confidence intervals in parentheses) of chromones **3-32** in radioligand binding assays at human  $A_1$ ,  $A_{2A}$ , and  $A_3$  adenosine receptor subtypes

Compound		$A_1$	$A_{2A}$	$A_3$	Selectivity	
		$K_i$ (nM)	$K_i$ (nM)	$K_i$ (nM)	$A_1/A_3$	$A_{2A}/A_3$
<b>3</b> <sup>26</sup>		> 100,000	> 100,000	14,200 (11,800-17,100)	>7.0	>7.0
<b>4</b> <sup>26</sup>		> 100,000	> 100,000	> 100,000	—	—
<b>5</b>		> 100,000	> 100,000	> 100,000	—	—
<b>6</b>		> 100,000	> 100,000	> 100,000	—	—
<b>7</b>		> 100,000	> 100,000	> 100,000	—	—
<b>8</b>		> 100,000	> 100,000	> 100,000	—	—
<b>9</b>		> 100,000	> 100,000	> 100,000	—	—
<b>10</b>		> 100,000	> 100,000	> 100,000	—	—
<b>11</b>		> 100,000	> 100,000	> 100,000	—	—
<b>12</b>		> 100,000	> 100,000	> 100,000	—	—
<b>13</b> <sup>26</sup>		> 100,000	> 100,000	15,800 (12,200-20,400)	>6.3	>6.3
<b>14</b> <sup>26</sup>		> 100,000	> 100,000	9,580 (7,600-12,100)	>10	>10
<b>15</b>		> 100,000	> 100,000	> 30,000	—	—
<b>16</b>		> 100,000	> 100,000	> 30,000	—	—
<b>17</b>		> 100,000	> 100,000	21,800 (17,300-27,500)	>4.5	>4.5
<b>18</b>		> 100,000	> 100,000	> 100,000	—	—
<b>19</b>		> 100,000	> 100,000	> 30,000	—	—
<b>20</b>		> 100,000	> 30,000	> 30,000	—	—
<b>21</b>		> 100,000	> 100,000	> 100,000	—	—
<b>22</b>		> 100,000	> 100,000	> 30,000	—	—
<b>23</b>		> 100,000	> 100,000	20,000 (16,500-24,300)	>5.0	>5.0
<b>24</b> <sup>26</sup>		> 100,000	> 100,000	27,900 (18,300-42,700)	>3.5	>3.5
<b>25</b>		> 100,000	> 100,000	> 100,000	—	—
<b>26</b>		> 100,000	> 100,000	> 100,000	—	—
<b>27</b>		10,200 (7,620-13,700)	18,900 (13,300-26,900)	10,700 (8,610-13,300)	0.96	1.8
<b>28</b>		12,000 (8,450-17,000)	18,500 (11,700-29,100)	> 100,000	<0.12	<0.18
<b>29</b>		17,300 (11,400-26,300)	15,100 (9,160-24,900)	11,900 (10,900-13,100)	1.4	1.3
<b>30</b>		8,180 (5,600-11,900)	10,400 (8,040-13,300)	1,310 (982-1,740)	6.3	7.9
<b>31</b>		> 100,000	> 80,000	167 (151-183)	>590	>480
<b>32</b>		> 100,000	> 100,000	4,780 (2,970-7,700)	>21	>21

The results obtained from the introduction of electron donating substituents in the exocyclic ring were not as straightforward as it was for the electron withdrawing groups. Preliminary data obtained in previous studies emphasizes the effect of electron donating groups located in *para* position of the exocyclic phenyl ring of the chromone-2-phenylcarboxamide (**3**) as it appear to modulate the affinity/selectivity for the A<sub>3</sub>AR.<sup>26</sup> From these studies one can highlight the data showing the influence of a *p*-methyl ( $K_i$ = 15,800 nM, compound **13**) and a *p*-methoxyl substituent ( $K_i$  = 9,580 nM compound **14**) on A<sub>3</sub>AR affinity (Table 1).<sup>26</sup> Hence, guided by this information it was decided to study the influence on affinity of the lengthening of the saturated carbon side chain, from one (-CH<sub>3</sub>, compound **13**), two (-C<sub>2</sub>H<sub>5</sub>, compound **15**) and four (-C<sub>4</sub>H<sub>9</sub>, compound **16**) carbon atoms. A complete loss of affinity towards all ARs subtypes was observed. These results suggest that the affinity of the chromone-2-phenylcarboxamides derivatives to ARs may be circumscribed by steric hindrance factors. Then, to assess the influence of the position of the electron donating substituent on the aromatic exocyclic nucleus, several positional isomers were synthesized. A decrease or absence of affinity was observed for substituents located either in *ortho* (CH<sub>3</sub>, compound **17**; OCH<sub>3</sub>, compound **19**) or *meta* (CH<sub>3</sub>, compound **18**; OCH<sub>3</sub>, compound **20**) positions. Noteworthy data was obtained by the isosteric replacement of the methoxyl group (compound **14**) by a thiomethyl (compound **21**) as it results in a compound with no affinity to all ARs. The effect of the presence of two electron donating substituents (-CH<sub>3</sub> and/or -OCH<sub>3</sub>) located in diverse positions (vicinal or meta position) of the exocyclic phenyl ring (compounds **22-26**) on ARs affinity was also inspected. A decrease (2,3-diCH<sub>3</sub>, compound **23** and 3,4-diOCH<sub>3</sub>, compound **24**) or no measurable affinity (3,4-diCH<sub>3</sub>, compound **22**) for the A<sub>3</sub>AR subtype was observed. Interestingly, the introduction of a *para* methoxyl and an *ortho* methyl substituents (2-CH<sub>3</sub>-4-OCH<sub>3</sub>, compound **25**) gave rise to an inactive compound. The same tendency has been previously observed with compound **24**, with two vicinal methoxy groups,<sup>26</sup> and compound **26** that possesses a methylenedioxy substituent on the exocyclic phenyl ring.

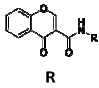
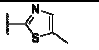
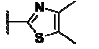
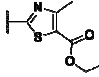
Our results reported here corroborate the preliminary SAR data observed in the previous studies.<sup>26</sup> In order to check the

reliability of the SAR studies, and taking into account the importance of the aromaticity of the carboxamide moiety for the affinity towards A<sub>3</sub>AR, a series of heterocyclic carboxamide derivatives were synthesised and evaluated towards all ARs subtypes (compounds **27-32**). In general, the introduction of a heterocyclic ring, directly linked to the NH of the carboxamide, resulted in active chromone-2-carboxamides with moderate to good binding affinities for human A<sub>1</sub>, A<sub>2A</sub> and A<sub>3</sub> ARs. However, the replacement of the phenyl (compound **3**,  $K_i$ = 14,200 nM) by an isosteric pyridine ring (compound **27**,  $K_i$ = 10,700 nM) or thiazol (compound **29**,  $K_i$ = 11,900 nM) gave rise to compounds with similar affinity towards A<sub>3</sub>ARs but a noticeable loss of selectivity was observed. Moreover, the presence of a CH<sub>2</sub> spacer between the carboxamide and the exoheterocyclic ring (compound **28**) led to a complete loss of affinity towards A<sub>3</sub>AR, although A<sub>1</sub> ( $K_i$ =12,000 nM) and A<sub>2A</sub> receptor ( $K_i$ =18,500 nM) binding affinities were detected. Inspiring results were obtained with the chromone-2-carboxamides bearing a substituted thiazolyl group (compounds **30-32**). The introduction of a methyl substituent at position 5 of the heterocyclic ring (compound **30**,  $K_i$ = 1,310 nM) gave rise to compounds about six- and eightfold selective for A<sub>3</sub> versus A<sub>1</sub> ( $K_i$ = 8,180 nM) and A<sub>2A</sub> ( $K_i$ = 10,400 nM) ARs, respectively. The introduction of an additional substituent at position 4 of the thiazol moiety (compounds **31** and **32**) led to even more selective and potent chromone-2-carboxamide derivatives. In fact, compound **31** was found to be the most potent and selective compound of all the chromone-2-carboxamide series tested so far, displaying a  $K_i$ = 167 nM for A<sub>3</sub>AR and selectivity ratios of 590 and 480 compared to A<sub>1</sub> and A<sub>2A</sub> ARs, respectively. The loss in potency observed with compound **32** (A<sub>3</sub>  $K_i$ = 4,780 nM) can be explained with the introduction of an electron withdrawing group (-COOEt) in the mentioned position.

The compelling results associated to the chromone-2-(thiazol-2-yl)carboxamides prompted to the synthesise of their positional C-3 isomers in order to corroborate the current SAR studies. The results for the binding affinity obtained for the chromone-3-(thiazol-2-yl)carboxamides (**33-35**) are summarized in Table 2.

In analogy to the C-2 isomers no measurable activity for A<sub>2B</sub> AR ( $K_i$  > 100,000 or 10,000 nM) was detected for the C-3

Table 2. Affinity ( $K_i$ , nM) of chromones **33-35** in radioligand binding assays at human A<sub>1</sub>, A<sub>2A</sub>, and A<sub>3</sub> adenosine receptor subtypes

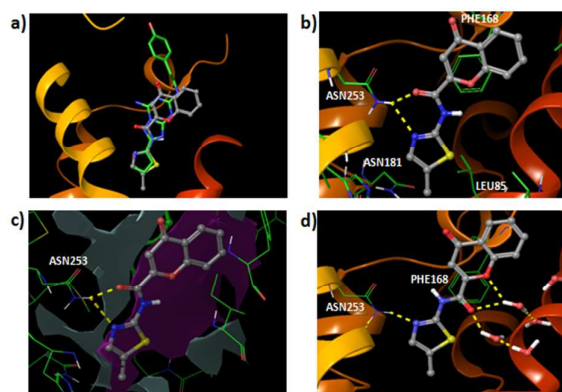
Compound		A <sub>1</sub>	A <sub>2A</sub>	A <sub>3</sub>	Selectivity	
		$K_i$ (nM)	$K_i$ (nM)	$K_i$ (nM)	A <sub>1</sub> /A <sub>3</sub>	A <sub>2A</sub> /A <sub>3</sub>
<b>33</b>		> 30,000	> 30,000	32,400 (25,100-41,800)	>0.9	>0.9
<b>34</b>		> 10,000	> 10,000	>10,000	—	—
<b>35</b>		> 10,000	> 10,000	10,000	—	—

carboxamides. From the analysed data it is possible to conclude that the position of the (thiazol-2-yl)carboxamide moiety at the chromone core is crucial for the observed affinity. In fact a decrease or a lack of affinity for all ARs was observed for compounds **33**, **34** and **35** that are positional isomers of compounds **30**, **31**, and **32**, respectively.

#### Molecular docking

Molecular docking simulations on  $hA_{2A}$  and  $hA_3$  receptors were performed to study the binding modes of the most active compounds in the series. To carry out this step, the crystal structure 3EML (PDB code)<sup>35</sup> for the  $hA_{2A}$  and a homology model for the  $hA_3$  ARs were used (see Experimental Section for more details).<sup>21</sup> The ligands were docked using Glide in the Schrodinger package.<sup>36</sup> For validation process the co-crystallized ligands ZM241385 and T4E in the structures 3EML<sup>35</sup> (including the role of water in the pocket) and 3UZC<sup>37</sup> were docked to the  $hA_{2A}$  protein. A RMSD (root mean square deviation) was obtained between the theoretical poses and the co-crystallized conformations of 0.69 and 1.92 for the ZM241385 and the triazine derivative T4E, respectively.

The docking calculations of chromone compounds showed a high degree of variability regarding possible binding modes in the pocket, in particular in the case of the  $hA_3$  homology model. Selection of the described binding modes was carried out taking into account the energetic parameter  $E_{\text{model}}$  and the number of similar poses yielded by the simulations. In both  $hA_{2A}$  and  $hA_3$  the active compounds with a thiazole ring (compounds **29** and **30**) shared a similar binding mode inside the AR subtype receptors. For instance compound **30** oriented the thiazole ring towards the bottom of the cavity whereas the chromone ring is placed closer to the extracellular environment in both receptors. The described binding mode presents some similarity to the co-crystallized antagonist ZM241385 in the  $hA_{2A}$  as it orientates the furan ring towards the bottom of the pocket in the same area as the thiazole ring of compound **30** (see Figure 4a). In the same manner as the co-crystallized ligand the compound established hydrogen bonds with the residue Asn253 of the  $hA_{2A}$  (see Figure 4b). Moreover, the hydrophobic/hydrophilic surface generated by the protein was also plotted. The surface revealed favored hydrophobic and hydrophilic areas for ligand interaction that can help to understand the pose of the compounds inside the protein. In fact, for compounds **29** and **30** a good accommodation for the thiazole ring was attained (see Figure 4c) whereas the introduction of a second 4-methyl substituent in the thiazole (compound **31**) lead to a loss of its fitting in the hydrophobic area. The loss of this hydrophobic interaction can cause the disruption of the binding mode being an important factor to explain the lack of affinity of compound **31** for the  $hA_{2A}$ AR ( $K_i > 80,000$  nM) compared to the derivatives **29** and **30** ( $K_i = 15,100$  nM and  $K_i = 10,400$  nM, respectively). Binding mode of compound **30** was also inspected by docking studies with water molecules present in the pocket of the crystallized structure 3EML. Compound **30** binding mode was similar as the one previously described. Thiazole ring pose is oriented towards the bottom of the cavity and established hydrogen

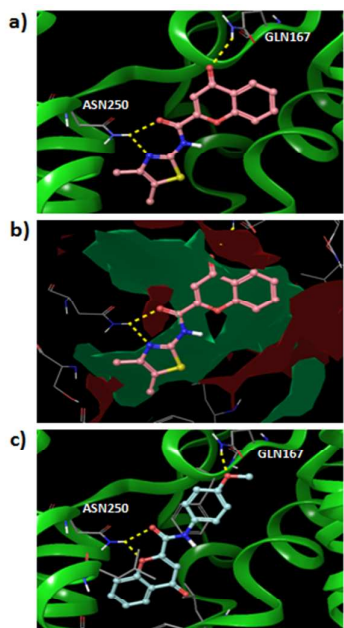


Figures 4. a) Comparison between the co-crystallized compound (green carbons) in the  $hA_{2A}$  (3EML) and the pose described by docking for compound **30** (grey carbons). b) Binding mode extracted from docking for compound **30** inside the  $hA_{2A}$  (protein in cartoon style). Hydrogen bonds are represented in yellow. c) Hydrophobic/hydrophilic surface generated inside the  $hA_{2A}$  (magenta color for hydrophobic and grey color for hydrophilic areas). d) Binding mode from docking for compound **30** in the  $hA_{2A}$  with water molecules in the pocket.

bonds with residue Asn253 and water molecules (see Figure 4d).

Thiazole chromone derivatives were also inspected in docking to the  $hA_3$  AR. The pose obtained for compound **31**, the most active compound in the series, is very similar to that obtained in the binding mode studies already described for the  $hA_{2A}$  (see Figure 5a). The analysis of the binding mode showed that the thiazole ring plays a key role in the anchoring of the amide moiety to the residue Asn250 through hydrogen bond interactions. Moreover, the oxygen of the carbonyl group in the chromone nucleus played an important role interacting with residue Gln167 of the second extracellular loop (EL2). In the case of the  $hA_{2A}$ , the residue Gln167 is not present as the protein contains a Leu in this position and so no hydrogen bond with the ligand is detected. This residue can be an operative feature in the ligand binding that can explain the enhanced affinity shown by the thiazole derivatives in the  $hA_3$ . On the other hand, hydrophobic/hydrophilic surfaces in the  $hA_3$  pocket showed important differences compared to the  $hA_{2A}$  in the area occupied by the thiazole ring. In the case of the  $hA_3$ , the hydrophobic surface is larger thus allowing hydrophobic substitutions at position 4 of the thiazole (see Figure 5b). This fact could explain the enhancement of  $hA_3$  activity of compound **31** ( $K_i = 167$  nM) with regard to derivatives **29** and **30** ( $K_i = 11,900$  nM and  $K_i = 1,310$  nM respectively). Moreover, the distinct hydrophobic distribution detected in both proteins ( $hA_{2A}$  and  $hA_3$ ) can elucidate the different adenosine selectivity of compound **31**.

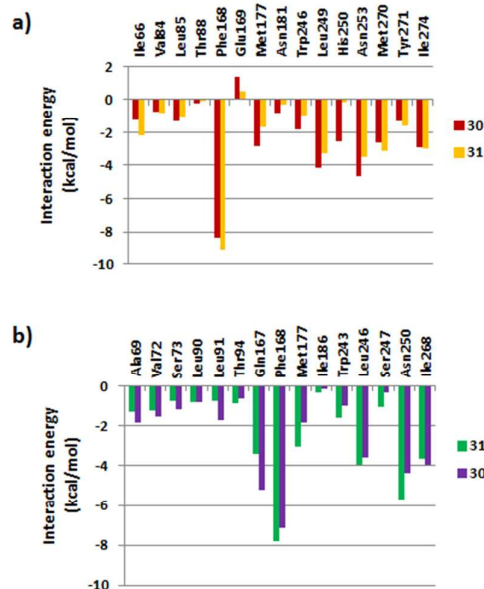
The  $hA_3$  also presents a favored hydrophobic surface close to the extracellular environment. As it was previously reported,<sup>38</sup> there are some differences in the extracellular loops of the  $hA_{2A}$  and  $hA_3$  that could determine not only the way how ligands bind to the protein but also modulate the entrance of ligands to the interior of the binding cavity. The different nature of some extracellular residues in both proteins, such as the hydrophobic Val169 in the  $hA_3$  and the ionic Glu169 in the



Figures 5. a) Pose for compound **31** in the  $hA_3$  determined by molecular docking. Hydrogen bonds are represented in yellow dashed lines and the protein in ribbon style. b) Hydrophobic/hydrophilic surface calculated in the  $hA_3$  (hydrophobic regions in green and hydrophilic domains in maroon). c) Binding mode calculated for compound **14** inside the  $hA_3$ . Hydrogen bonds with residues Asn250 and Gln167 are represented in yellow color.

$hA_{2A}$ , could influence the access and accommodation of the ligands. Introduction of a second methyl in the thiazole fragment contributed to an increase of  $hA_3$  activity as the receptor present a deeper hydrophobic surface.

Moreover, the contribution to the interaction energy of the different residues placed in a distance of 4 Å from the ligand in the  $hA_{2A}$  and  $hA_3$  was calculated. The interaction energy (Figure 6) was calculated as the sum of three scores: Coulomb, *van der Waals* and hydrogen bonding. Compound **30** inside the  $hA_{2A}$  interacts preferably with residues Phe168, Asn253, Leu249, Ile274 and Met177. Although compound **31** presents a similar interaction outline a lower interaction with residue His250 was noticed. The important role of some residues in ligand binding, such as Phe168, Asn253, Leu249 or Met177 was previously confirmed in mutagenesis studies that examined the effect of mutating residues in  $hA_{2A}$  activity.<sup>38</sup> On the other hand, and using the same approach, the most important residues in the interaction between compounds **30-**



Figures 6. Residue interaction energy scores between  $hA_{2A}$  and compounds **30-31** (panel a) and  $hA_3$  and compounds **30-31** (panel b). Interaction energy is calculated as the sum of Coulomb, *van der Waals* and hydrogen bonding energies.

**31** and the  $hA_3$  were determined: Phe168, Asn250, Leu246, Ile268 and Gln167. The higher interaction of compound **31** with the key residue Asn250 can also validate its superior  $hA_3$  activity. It is noteworthy that although  $hA_3$  possesses high identity with the  $hA_{2A}$  there are also differences in some residues of the binding pocket which can condition the binding of the different ligands.

The position of the carboxamide in the chromone ring was also found to be important for  $A_3$  adenosine receptor affinity. In fact, compounds with the carboxamide function at position 3, such as compound **34**, showed a drastic loss of  $hA_3$  activity. Docking calculations in  $hA_3$  regarding compound **34** demonstrated a hypothetical binding mode with the chromone ring in a similar position as the one described for compound **31**. However, compound **34** oriented the carboxamide substituent towards the extracellular environment. The different binding mode could be responsible for the loss of  $hA_3$  activity.

In addition, molecular modeling studies were performed with the chromone-2-phenylcarboxamide with a methoxyl substituent located in *para* position of the exocyclic aromatic ring (**14**). It was concluded that this type of chromone presented a different binding mode in the  $hA_3AR$  (see Figure 5c). Compound **14** oriented the chromone scaffold towards the bottom of the cavity and the *para*-methoxyphenyl moiety towards the extracellular region through the interaction of hydrogen bonds with residues Asn250 and Gln167. Similar binding modes for this type of chromone-2-phenylcarboxamide derivatives were previously reported by our research group.<sup>26</sup> So, aromatic heterocyclic systems are considered to be positive bioisosteric replacements to improve  $hA_3AR$  affinity of this type of ligands.



From the overall studies one can conclude that the hydrophobic area in the extracellular environment due to the presence of hydrophobic residues, such as Val169 and Leu264, can be considered a significant feature to be accomplished along compound **31** optimization subsequent step. The change of the type of heterocycle is considered to be an important approach to obtain additional information, improve the affinity and validate the docking studies. Also the presence of other type of electron donator substituents, which must be oriented toward the extracellular area, must be explored.

Scoring function energies for each compound docked to the  $hA_{2A}$  and  $hA_3$  are shown in Table 3. From the data one can conclude that molecular docking showed limited ability to discriminate active from non-active compounds, even though the results are variable depending on the scoring function (SP or XP) and the adenosine subtype. SP (standard precision) scoring function showed better discriminatory power than the XP (extra-precision) scoring. The area under the ROC curves (AUROC) was also calculated to evaluate the discriminatory ability in the series. SP scoring showed AUROCs of 0.77 and 0.64 in the  $hA_{2A}$  (including water or not in the pocket). The most  $hA_{2A}$  active compound (**30**) in the series is identified by the SP models in position 2 and 8, respectively. Docking in  $hA_3$  showed more limitations to differentiate between active and non-active compounds. However,  $hA_3$  docking with SP function showed some ability to capture the most active compounds in the series in top positions (positions 9, 10, 13, 15 and 16 for compounds **30**, **32**, **14**, **31** and **35** respectively). AUROC is 0.66 considering as actives the compounds with  $K_i \leq 10,000$  nM. Docking studies showed some limitations from the energetic point of view in the  $hA_{2A}$  crystal structure and the  $hA_3$  homology model.

	$hA_{2A}$		$hA_{2A}$		$hA_3$	
	SP (no water)	XP (no water)	SP (water)	XP (water)	SP (no water)	XP (no water)
AUROC	0.64	0.47	0.77	0.66	0.66	0.36
Comp.	SP (no water)	XP (no water)	SP (water)	XP (water)	SP (no water)	XP (no water)
<b>3</b>	-7.80	-8.33	-7.27	-6.95	-7.78	-7.06
<b>4</b>	-6.61	-8.62	-7.56	-6.79	-8.48	-8.22
<b>5</b>	-7.60	-7.72	-7.75	-6.28	-7.93	-7.56
<b>6</b>	-6.81	-7.82	-7.09	-6.39	-8.30	-7.87
<b>7</b>	-7.16	-7.56	-6.76	-5.98	-7.28	-7.46
<b>8</b>	-7.80	-8.60	-6.10	-5.08	-9.01	-8.19
<b>9</b>	-6.32	-9.07	-6.77	-6.15	-8.68	-7.47
<b>10</b>	-7.53	-7.53	-6.51	-6.40	-8.62	-7.42
<b>11</b>	-8.37	-8.30	-5.46	-5.23	-7.54	-9.49
<b>12</b>	-7.23	-8.66	-7.68	-7.74	-7.93	-7.69
<b>13</b>	-7.69	-8.28	-7.49	-6.33	-7.65	-8.05
<b>14</b>	-7.83	-8.37	-5.13	-5.95	-8.35	-8.10
<b>15</b>	-7.58	-7.86	-6.74	-6.67	-8.30	-7.77
<b>16</b>	-5.94	-9.45	-5.47	-5.24	-8.66	-8.40
<b>17</b>	-6.84	-3.70	-7.12	-6.85	-7.97	-7.49
<b>18</b>	-7.43	-8.58	-7.76	-7.64	-7.82	-8.01
<b>19</b>	-5.82	-8.71	-7.62	-6.87	-8.03	-7.98
<b>20</b>	-7.72	-8.60	-6.14	-5.11	-8.44	-7.94
<b>21</b>	-7.64	-7.32	-6.38	-5.84	-7.86	-7.32
<b>22</b>	-8.31	-8.70	-8.19	-6.62	-8.40	-8.48
<b>23</b>	-6.89	-8.73	-7.18	-6.26	-8.29	-8.13
<b>24</b>	-6.76	-5.43	-5.94	-6.22	-8.62	-8.77
<b>25</b>	-7.11	-8.86	-5.62	-5.36	-8.71	-9.04
<b>26</b>	-7.13	-6.84	-6.40	-7.21	-8.32	-7.82
<b>27</b>	-7.57	-9.77	-6.34	-6.52	-8.57	-6.80

<b>28</b>	-7.54	-8.09	-7.88	-7.28	-8.29	-7.91
<b>29</b>	-7.46	-6.44	-7.94	-6.50	-8.11	-6.60
<b>30</b>	-7.72	-7.88	-8.31	-7.14	-8.45	-6.29
<b>31</b>	-7.50	-7.85	-8.38	-7.21	-8.32	-7.08
<b>32</b>	-6.83	-8.11	-6.10	-7.15	-8.44	-7.76
<b>33</b>	-7.73	-7.89	-7.65	-7.34	-7.55	-7.37
<b>34</b>	-6.57	-8.17	-8.13	-7.58	-7.14	-7.87
<b>35</b>	-7.06	-7.49	-6.25	-7.21	-8.31	-7.96

SP (standard precision scoring function), XP (extra-precision scoring function, kcal/mol). For AUROC calculation, compounds **27-30** were actives in the  $hA_{2A}$ , and compounds **14**, **30**, **31**, **32** and **35** were actives in the  $hA_3$  ( $K_i \leq 10,000$  nM). Calculations with and without water molecules in the  $hA_{2A}$  pocket were performed.

## Conclusions

The search for novel compounds with therapeutic value by targeting  $A_3$  ARs is still in its infancy and additional research in the field is still needed. The role of  $A_3$ AR agonists and antagonists is still an open issue and the development of new and superior agonists/antagonists that can reach clinical trials remains an emergent topic. Previous research performed by our group has shown that chromone-2-phenylcarboxamide is a valid scaffold for tracking novel ligands with affinity for  $A_3$ AR. Thus, the study presented here provides new insights into the SAR regarding the chromone-2-phenylcarboxamide framework. This input, supported by  $A_{2A}/A_3$  molecular docking simulations and structure-affinity-relationship (SAR) studies, lead to the identification of the crucial role for  $A_3$ AR affinity of a heteroamide substituent located at C-2 of the pyrone ring. The most remarkable chromone-2-carboxamides with affinity towards  $A_3$ ARs were compounds **30**, **31** and **32** with  $K_i$  values of 1,310 nM, 167 nM and 4,780 nM, respectively. Compound **31**, displaying an  $A_3$   $K_i$  of 167 nM and a selectivity ratio of 590 vs. the  $A_1$  and 480 vs. the  $A_{2A}$ AR subtypes, stood out as the best chromone derivative tested so far, showing an enhanced  $A_3$ AR affinity and selectivity compared to the flavonoids presently known. Moreover, compound **31** present appealing drug-like properties (e.g. clogP 2.44 and molecular polar surface area of 72.20) and no violations of Lipinski rule.

In addition, the present study supports the belief that chromone due to its synthetic accessibility and decoration capability, is a privileged structure for the design and development of libraries in the discovery of novel and innovative ARs ligands. Finally, the receptor-driven molecular modeling studies have provided valuable information on the molecular interactions responsible for selective high affinity binding to the  $A_3$  adenosine receptor of the most promising chromones. In this respect the data are instrumental for future optimization of potency and drug-like properties of chromone-2-(hetero)carboxamides.

## Experimental section

### Chemistry

Chromone-2-carboxylic acid, benzotriazol-1-yloxy)tripyrrolidinophosphonium hexafluorophosphate

(PyBOP), *N,N*-diisopropylethylamine (DIPEA), dimethylformamide (DMF), phosphoryl trichloride (POCl<sub>3</sub>), arylamines and heteroamines were purchased from Sigma-Aldrich Química S.A. (Sintra, Portugal). All other reagents and solvents were *pro analysis* grade and were acquired from Merck (Lisbon, Portugal), Panreac (Lisbon, Portugal) and Sigma Aldrich (Sintra, Portugal), used without additional purification. Thin-layer chromatography (TLC) was carried out on pre-coated silica gel 60 F254 (Merck) with layer thickness of 0.2 mm. The spots were visualized under UV detection (254 and 366 nm) and iodine vapour. Normal-phase column chromatography was performed using silica gel 60 0.2-0.5 or 0.040-0.063 mm (Merck).

Following the workup and after extraction, the organic phases were dried over Na<sub>2</sub>SO<sub>4</sub>. Solutions were decolorized with activated charcoal, when necessary. Solvents were evaporated in a Buchi Rotavapor.

The purity of the final products (>97% purity) was verified by high-performance liquid chromatography (HPLC) equipped with a UV detector. Chromatograms were obtained in an HPLC/DAD system, a Jasco instrument (pumps model 880-PU and solvent mixing model 880-30, Tokyo, Japan), equipped with a commercially prepacked RP-18 analytical column (250 mm x 4.6 mm, 5 μm, Macherey-Nagel, Duren, Germany), and UV detection (Jasco model 875-UV) at the maximum wavelength of 254 nm. The mobile phase consisted of a methanol/water or acetonitrile/water (gradient mode, room temperature) at a flow rate of 1 mL/min. The chromatographic data was processed in a Compaq computer, fitted with CSW 1.7 software (DataApex, Czech Republic).

**Apparatus.** The main paragraph text <sup>1</sup>H NMR and <sup>13</sup>C NMR data were acquired, at room temperature, on a Bruker AMX 400 spectrometer operating at 400.15 and 101.0 MHz, respectively. Chemical shifts are expressed in δ (ppm) values relative to tetramethylsilane (TMS) as internal reference; coupling constants (*J*) are given in Hz. Electron impact mass spectra (EI-MS) were carried out on a VG AutoSpec instrument; the data are reported as *m/z* (% of relative intensity of the most important fragments).

**Synthesis.** The chromone derivatives were synthesised by two synthetic approaches previously developed by our group.<sup>28,29</sup>

**Method A:** To a solution of the chromone-2-carboxylic acid or chromone-3-carboxylic (1.1 mmol) in DMF (2.5 mL) at 4 °C it was added was added *N,N*-diethylpropan-2-amine (1.1 mmol) and a solution of PyBOP (1mmol) in CH<sub>2</sub>Cl<sub>2</sub> (2.5 mL). The mixture was kept in an ice bath and stirred for half hour. After this period the amine with the desired (hetero)aromatic pattern was added and the mixture was allowed to warm up to room temperature. The reaction was kept under stirring for 4 hours. The working-up of the crude material enclosed a liquid-liquid extraction CH<sub>2</sub>Cl<sub>2</sub> followed by flash chromatography (CH<sub>2</sub>Cl<sub>2</sub>/MeOH or EtOAc/*n*-hexane) and final purification by recrystallization (EtOAc/*n*-hexane).

*N*-phenyl-4-oxo-4*H*-chromene-2-carboxamide (**3**): the synthetic procedure and structural elucidation data was described elsewhere.<sup>44</sup>

*N*-(4-chlorophenyl)-4-oxo-4*H*-chromene-2-carboxamide (**4**): the synthetic procedure and structural elucidation data was described elsewhere.<sup>45</sup>

*N*-(4-Fluorophenyl)-4-oxo-4*H*-chromene-2-carboxamide (**5**): Yield: 75%. <sup>1</sup>H NMR (DMSO-D<sub>6</sub>): δ = 6.98 (1H, *s*, H(3)), 7.28 (2H, *dd*, *J* = 8.9, H(3'), H(5')), 7.57 (1H, *ddd*, *J* = 8.0, 7.0, 1.0, H(6)), 7.81-7.85 (3H, *m*, H(8), H(2'), H(6')), 7.94 (1H, *ddd*, *J* = 1.6, 7.0, 8.6, H(7)), 8.09 (1H, *dd*, *J* = 1.6, 8.0, H(5)), 10.81 (1H, *s*, CONH). <sup>13</sup>C NMR (DMSO-D<sub>6</sub>): δ = 112.5 (C(3)), 116.9 (*d*, *J* = 22.5, C(3'), C(5')), 120.4 (C(8)), 124.5 (*d*, *J* = 8.2, C(2'), C(6')), 125.1 (C(4a)), 126.3 (C(6)), 127.5 (C(5)), 135.2 (C(7)), 136.5 (C(1')), 156.5 (C(8a)), 157.0 (CONH), 159.1 (C(2)), 160.4 (*d*, *J* = 241.9, C(4')) 178.7 (C(4)). *EM/IE m/z*: 284 (M+1, 21), 283 (M<sup>+</sup>, 100), 282 (83), 254 (29), 145 (23), 89 (58).

*N*-(4-Bromophenyl)-4-oxo-4*H*-chromene-2-carboxamide (**6**): the synthetic procedure and structural elucidation data was described elsewhere.<sup>28</sup>

*N*-(4-Iodophenyl)-4-oxo-4*H*-chromene-2-carboxamide (**7**) Yield: 95% <sup>1</sup>H NMR (DMSO-D<sub>6</sub>): δ = 6.97 (1H, *s*, H (3)), 7.56 (1H, *ddd*, *J* = 1.0, 7.1, 8.0, H(6)), 7.65 (2H, *d*, *J* = 8.8, H(3'), H(5')), 7.77 (2H, *d*, *J* = 8.8, H(2'), H(6')), 7.84 (1H, *d*, *J* = 8.5, H(8)), 7.93 (1H, *ddd*, *J* = 1.6, 7.0, 8.6, H(7)), 8.08 (1H, *dd*, *J* = 1.4, 8.0, H(5)), 10.82 (1H, *s*, NH). <sup>13</sup>C NMR (DMSO-D<sub>6</sub>): δ = 90.5 (C(4')), 112.6 (C(3)), 120.4 (C(8)), 124.5 (C(2'), C(6')), 124.6 (C(4a)), 126.3 (C(6)), 127.5 (C(5)), 136.5 (C(7)), 138.8 (C(1')), 138.9 (C(3'), C(5')), 156.5 (C(8a)), 156.8 (C(2)), 159.2 (NH), 178.6 (C(4)). *MS/EI m/z*: 392 (22), 391 (M<sup>+</sup>, 100), 390 (47), 362 (16), 145 (13), 89 (45), 86 (12), 84 (18), 70 (10).

*N*-(4-Acetylphenyl)-4-oxo-4*H*-chromene-2-carboxamide (**8**): <sup>1</sup>H NMR (CDCl<sub>3</sub>): δ = 2.66 (3H, *s*, CH<sub>3</sub>), 7.38 (1H, *s*, H(3)), 7.55 (1H, *app t*, *J* = 7.8, H(6)), 7.78 (1H, *d*, *J* = 8.6, H (8)), 7.85 (1H, *ddd*, *J* = 1.5, 7.8, 8.0, H(7)), 7.95 (2H, *d*, *J* = 8.7, H(3'), H(5')), 8.06 (2H, *d*, *J* = 8.7, H(2'), H(6')), 8.26 (1H, *dd*, *J* = 7.8, 1.5, H(5)), 9.86 (1H, *s*, CONH). <sup>13</sup>C NMR (CDCl<sub>3</sub>): δ = 26.4 (CH<sub>3</sub>), 112.4 (C(3)), 118.4 (C(8)), 120.2 (C(3'), C(5')), 124.1 (C(4a)), 125.9 (C(5)), 126.3 (C(6)), 129.7 (C(2'), C(6')) 133.7 (C(1')), 135.1 (C(7)), 141.3 (C(4')), 154.9 (C(8a)), 155.5 (C(2)), 157.8 (CONH), 178.7 (C(4)), 197.8 (COCH<sub>3</sub>). *MS/EI m/z*: 307 (M<sup>+</sup>, 87), 292 (100), 146 (19), 121 (37), 89 (56).

*N*-(4-Ethoxycarbonylphenyl)-4-oxo-4*H*-chromene-2-carboxamide (**9**): Yield: 82 %. <sup>1</sup>H NMR (CDCl<sub>3</sub>): δ = 1.41 (3H, *t*, *J* = 7.1, CH<sub>2</sub>CH<sub>3</sub>), 4.39 (2H, *d*, *J* = 7.1, CH<sub>2</sub>CH<sub>3</sub>), 7.28 (1H, *s*, H(3)), 7.50 (1H, *ddd*, *J* = 1.0, 7.1, 8.0, H(6)), 7.61 (1H, *d*, *J* = 8.5, H(8)), 7.79 (1H, *ddd*, *J* = 1.6, 7.0, 8.6, H(7)), 7.82 (2H, *d*, *J* = 8.8, H(3'), H(5')), 8.11 (2H, *d*, *J* = 8.8, H(2')), H(6')), 8.25 (1H, *dd*, *J* = 1.4, 8.0, H(5)), 8.74 (1H, *s*, CONH). <sup>13</sup>C NMR (CDCl<sub>3</sub>): δ = 14.3 (CH<sub>2</sub>CH<sub>3</sub>), 61.1 (CH<sub>2</sub>CH<sub>3</sub>), 112.9 (C(3)), 118.0 (C(8)), 119.5 (C(2'), C(6')), 123.9 (C(4a)), 124.3 (C(4')), 126.3 (C(6)), 127.4 (C(5)), 130.9 (C(3'), C(5')), 134.8 (C(7)), 140.3 (C(1')), 154.1 (C(8a)), 155.1 (C(2)), 157.1 (CONH), 177.0 (C(4)). *EM/IE m/z*: 338 (37), 337 (94), 336 (M<sup>+</sup>, 100), 320 (24), 309 (13), 308 (53), 293 (18),

292 (81), 280 (14), 265 (17), 264 (18), 146 (17), 145 (18), 121 (29), 120 (12), 101 (12), 89 (63).

*N*-(4-Cyanophenyl)-4-oxo-4*H*-chromene-2-carboxamide (**10**): Yield: 71%.  $^1\text{H NMR}$  (DMSO- $D_6$ ):  $\delta$  = 7.01 (1H, *s*, H(3)), 7.56 (1H, *ddd*,  $J$  = 1.2, 7.4, 7.8, H(6)), 7.82 – 7.87 (3H, *m*, H(3'), H(5'), H(8)), 7.93 (1H, *ddd*,  $J$  = 1.6, 7.6, 8.0, H(7)), 7.98 (2H, *d*,  $J$  = 8.8, H(2'), H(6')), 8.08 (1H, *dd*,  $J$  = 1.2, 8.0, H(5)), 11.09 (1H, *s*, NH).  $^{13}\text{C NMR}$  (DMSO- $D_6$ ):  $\delta$  = 105.3 (C(4')), 110.6 (C(3)), 110.7 (CN), 118.4 (C(2'), C(6')), 121.0 (C(8)), 123.1 (C(4a)), 124.3 (C(6)), 125.5 (C(5)), 132.5 (C(3')), C(5')), 134.4 (C(7)), 143.1 (C(1')), 154.6 (C(8a)), 155.6 (C(2)), 158.2 (NH), 176.7 (C(4)). *MS/EI m/z*: 290 ( $M^{+}$ , 91), 289 (100), 261 (25), 173 (26), 145 (39), 89 (88), 69 (20).

*N*-(2-Chlorophenyl)-4-oxo-4*H*-chromene-2-carboxamide (**11**): the synthetic procedure and structural elucidation data was described elsewhere.<sup>39</sup>

*N*-(3-Chlorophenyl)-4-oxo-4*H*-chromene-2-carboxamide (**12**): the synthetic procedure and structural elucidation data was described elsewhere.<sup>39</sup>

*N*-(*p*-Tolyl)-4-oxo-4*H*-chromene-2-carboxamide (**13**): the synthetic procedure and structural elucidation data was described elsewhere.<sup>26</sup>

*N*-(4-methoxyphenyl)-4-oxo-4*H*-chromene-2-carboxamide (**14**): the synthetic procedure and structural elucidation data was described elsewhere.<sup>26</sup>

*N*-(4-Ethylphenyl)-4-oxo-4*H*-chromene-2-carboxamide (**15**): Yield: 67%.  $^1\text{H NMR}$  ( $\text{CDCl}_3$ ):  $\delta$  = 1.24 (3H, *t*,  $J$  = 7.6,  $\text{CH}_3$ ), 2.65 (2H,  $J$  = 7.6,  $\text{CH}_2$ ), 7.23 (2H, *d*,  $J$  = 8.5, H(3')), H(5')), 7.25 (1H, *s*, H(3)), 7.47 (1H, *ddd*,  $J$  = 1.0, 7.2, 8.0, H(6)), 7.57-7.65 (3H, *m*, H(8), H(2'), H(6')), 7.76 (1H, *ddd*,  $J$  = 1.5, 7.2, 8.7, H(7)), 8.23 (1H, *dd*,  $J$  = 1.5, 8.0, H(5)), 8.55 (1H, *s*, NH).  $^{13}\text{C NMR}$  ( $\text{CDCl}_3$ ):  $\delta$  = 15.5 ( $\text{CH}_3$ ), 28.4 ( $\text{CH}_2$ ), 112.3 (C(3)), 118.1 (C(8)), 120.6 (C(2'), C(6')), 124.4 (C(4a)), 126.1 (C(6)), 126.2 (C(5)), 128.6 (C(3'), C(5')), 134.0 (C(4')), 134.7 (C(7)), 142.0 (C(1')), 154.7 (C(8a)), 155.2 (C(2)), 156.8 (CONH), 178.0 (C(4)). *MS/EI m/z*: 293 ( $M^{+}$ , 100), 278 (20), 264 (20), 120 (31), 107 (23), 89 (99), 77 (25).

*N*-(4-Butylphenyl)-4-oxo-4*H*-chromene-2-carboxamide (**16**): Yield: 69%.  $^1\text{H NMR}$  ( $\text{CDCl}_3$ ):  $\delta$  = 0.93 (3H, *t*,  $J$  = 7.3,  $\text{CH}_3$ ), 1.31-1.41 (2H, *m*,  $\text{CH}_2$ ), 1.59-1.62 (2H, *m*,  $\text{CH}_2$ ), 2.61 (2H, *t*,  $J$  = 7.7,  $\text{CH}_2$ ), 7.21 (2H, *d*,  $J$  = 8.5, H(3'), H(5')), 7.26 (1H, *s*, H(3)), 7.48 (1H, *ddd*,  $J$  = 1.0, 7.2, 8.1, H(6)), 7.57-7.63 (3H, *m*, H(8), H(2'), H(6')), 7.77 (1H, *ddd*,  $J$  = 1.6, 7.2, 8.5, H(7)), 8.24 (1H, *dd*,  $J$  = 1.6, 8.1, H(5)), 8.55 (1H, *s*, NH).  $^{13}\text{C NMR}$  ( $\text{CDCl}_3$ ):  $\delta$  = 13.9 ( $\text{CH}_3$ ), 22.3 ( $\text{CH}_2$ ), 33.5 ( $\text{CH}_2$ ), 35.1 ( $\text{CH}_2$ ), 112.5 (C(3)), 118.1 (C(8)), 120.5 (C(2'), C(6')), 124.4 (C(4a)), 126.1 (C(6)), 126.2 (C(5)), 129.2 (C(3'), C(5')), 133.9 (C(4')), 140.6 (C(1')), 134.4 (C(7)), 154.7 (C(8a)), 155.2 (C(2)), 156.8 (CONH), 178.1 (C(4)). *MS/EI m/z*: 321 ( $M^{+}$ , 81), 278 (100), 107 (68), 89 (88).

*N*-(2-Methylphenyl)-4-oxo-4*H*-chromene-2-carboxamide (**17**): the synthetic procedure and structural elucidation data was described elsewhere.<sup>39</sup>

*N*-(3-Methylphenyl)-4-oxo-4*H*-chromene-2-carboxamide (**18**): the synthetic procedure and structural elucidation data was described elsewhere.<sup>39</sup>

*N*-(4-(Methylthio)phenyl)-4-oxo-4*H*-chromene-2-carboxamide (**21**): the synthetic procedure and structural elucidation data was described elsewhere.<sup>40</sup>

*N*-(3,4-Dimethylphenyl)-4-oxo-4*H*-chromene-2-carboxamide (**22**): Yield: 75%  $^1\text{H NMR}$  (DMSO- $D_6$ ):  $\delta$  = 2.21 (3H, *s*,  $\text{CH}_3$ ), 2.24 (3H, *s*,  $\text{CH}_3$ ), 6.95 (1H, *s*, H(3)), 7.16 (1H, *d*,  $J$  = 8.0, H(5')), 7.52-7.54 (1H, *m*, H(2')), 7.56-7.58 (2H, *m*, H(6'), H(6)), 7.84 (1H, *d*,  $J$  = 8.0, H(8)), 7.93 (1H, *ddd*,  $J$  = 1.2, 6.8, 8.0, H(7)), 8.08 (1H, *dd*,  $J$  = 1.2, 8.0, H(5)), 10.60 (1H, *s*, NH).  $^{13}\text{C NMR}$  (DMSO- $D_6$ ):  $\delta$  = 20.3 ( $\text{CH}_3$ ), 21.0 ( $\text{CH}_3$ ), 112.3 (C(3)), 119.9 (C(8)), 121.4 (C(2')), 123.5 (C(6)), 125.1 (C(4a)), 126.3 (C(6')), 127.5 (C(5)), 131.0 (C(3')), 134.3 (C(4'), C(5')), 136.4 (C(7)), 137.9 (C(1')), 156.5 (C(8a)), 157.2 (C(2)), 158.8 (CONH), 178.7 (C(4)). *MS/EI m/z*: 293 ( $M^{+}$ , 100), 292 (90), 276 (25), 264 (35), 173 (22), 120 (45), 89 (49), 77 (24).

*N*-(3,4-Dimethoxyphenyl)-4-oxo-4*H*-1-benzopyran-2-carboxamide (**24**): the synthetic procedure and structural elucidation data was described elsewhere.<sup>26</sup>

*N*-(Benzodioxol-5-yl)-4-oxo-4*H*-chromene-2-carboxamide (**26**): Yield: 62%.  $^1\text{H NMR}$  (DMSO- $D_6$ ):  $\delta$  = 6.05 (2H, *s*,  $\text{CH}_2$ ), 6.95 (1H, *s*, H(3)), 6.97 (1H, *d*,  $J$  = 8.4, H(5')), 7.24 (1H, *dd*,  $J$  = 2.4, 8.4, H(6')), 7.43 (1H, *d*,  $J$  = 2.4, H(2')), 7.57 (1H, *ddd*,  $J$  = 1.0, 7.6, 9.2, H(6)), 7.84 (1H, *dd*,  $J$  = 0.8, 8.4, H(8)), 7.93 (1H, *app dt*,  $J$  = 1.6, 7.8, H(7)), 8.08 (1H, *dd*,  $J$  = 1.6, 8.0, H(5)), 10.65 (1H, *s*, NH).  $^{13}\text{C NMR}$  (DMSO- $D_6$ ):  $\delta$  = 100.7 ( $\text{CH}_2$ ), 102.4 (C(2')), 107.5 (C(5')), 110.4 (C(6')), 113.8 (C(3)), 118.4 (C(8)), 123.1 (C(4a)), 124.4 (C(6)), 125.5 (C(5)), 131.1 (C(1')), 134.5 (C(7)), 143.7 (C(4')), 146.5 (C(3')), 154.6 (C(8a)), 155.1 (C(2)), 156.8 (NH), 176.7 (C(4)). *MS/EI m/z*: 310 ( $M^{+}$ , 25), 309 ( $M^{+}$ , 100), 292 (17), 280 (18), 189 (30), 136 (65), 89 (33).

*N*-(Pyridin-2-yl)-4-oxo-4*H*-chromene-2-carboxamide (**27**): Yield: 31%.  $^1\text{H NMR}$  ( $\text{CDCl}_3$ ):  $\delta$  = 7.19 (1H, *ddd*,  $J$  = 0.9, 5.0, 7.4, H(4')), 7.30 (1H, *s*, H(3)), 7.50 (1H, *ddd*,  $J$  = 1.0, 7.2, 8.1, H(6)), 7.63 (1H, *dd*,  $J$  = 0.6, 8.5, H(6')), 7.89-7.72 (2H, *m*, H(5'), H(8)), 8.25 (1H, *dd*,  $J$  = 1.4, 8.0, H(3')), 8.45-8.32 (2H, *m*, H(5), H(7)), 9.31 (1H, *s*, NH).  $^{13}\text{C NMR}$  ( $\text{CDCl}_3$ ):  $\delta$  = 113.0 (C(3)), 114.8 (C(6')), 118.2 (C(8)), 121.1 (C(4')), 124.4 (C(4a)), 126.2 (C(6)), 126.3 (C(5)), 134.9 (C(7)), 139.0 (C(5')), 148.1 (C(3')), 150.1 (C(1')), 154.0 (C(8a)), 155.2 (C(2)), 157.3 (CONH), 177.9 (C(4)). *MS/EI m/z*: 267 (22), 266 ( $M^{+}$ , 99), 238 (58), 237 (66), 210 (83), 89 (100).

*N*-(Furan-2-ylmethyl)-4-oxo-4*H*-chromene-2-carboxamide (**28**): Yield: 35%.  $^1\text{H NMR}$  ( $\text{CDCl}_3$ ):  $\delta$  = 4.68 (2H, *d*,  $J$  = 5.7,  $\text{CH}_2$ ), 6.42-6.32 (2H, *m*, H(4'), H(5')), 7.19 (1H, *s*, H(3)), 7.23 (1H, *bs*, NH), 7.42 (1H, *dd*,  $J$  = 0.9, 1.7, H(3')), 7.48-7.43 (1H, *m*, H(6)), 7.52 (1H, *dd*,  $J$  = 0.5, 8.5, H(8)), 7.73 (1H, *ddd*,  $J$  = 1.7, 7.2, 8.7, H(7)), 8.22 (1H, *dd*,  $J$  = 1.4, 8.0, H(5)).  $^{13}\text{C NMR}$  ( $\text{CDCl}_3$ ):  $\delta$  = 36.9 ( $\text{CH}_2$ ), 108.6 (C(5')), 110.8 (C(4')), 112.5 (C(3)), 118.2 (C(8)), 124.4 (C(4a)), 126.1 (C(6)), 126.2 (C(5)), 134.7 (C(7)), 142.8 (C(3')), 150.1 (C(1')), 154.6 (C(8a)), 156.3 (C(2)), 159.2 (CONH), 178.2 (C(4)). *MS/EI m/z*: 270 (22), 269 ( $M^{+}$ , 100), 297 (11), 146 (21), 145 (16).

*N*-(Thiazol-2-yl)-4-oxo-4*H*-chromene-2-carboxamide (**29**): Yield: 55%. <sup>1</sup>H NMR (CDCl<sub>3</sub>): δ = the synthetic procedure and structural elucidation data was described elsewhere.<sup>41</sup>

*N*-(5-Methylthiazol-2-yl)-4-oxo-4*H*-chromene-2-carboxamide (**30**): the synthetic procedure and structural elucidation data was described elsewhere.<sup>41</sup>

*N*-(4,5-dimethylthiazol-2-yl)-4-oxo-4*H*-chromene-2-carboxamide (**31**): the synthetic procedure and structural elucidation data was described elsewhere.<sup>41</sup>

Ethyl 4-methyl-2-(4-oxo-4*H*-chromene-3-carboxamido)thiazole-5-carboxylate (**35**): yield: 15%. <sup>1</sup>H NMR (CDCl<sub>3</sub>): δ = 1.37 (3H, *t*, *J* = 7.1, OCH<sub>2</sub>CH<sub>3</sub>), 2.69 (3H, *s*, CH<sub>3</sub>), 4.33 (2H, *q*, *J* = 7.1, OCH<sub>2</sub>CH<sub>3</sub>), 7.57 (1H, *m*, H(6)), 7.61 (1H, *d*, *J* = 8.4, H(8)), 7.82 (1H, *ddd*, *J* = 1.6, 7.3, 8.6, H(7)), 8.37 (1H, *dd*, *J* = 1.6, 8.0, H(5)), 9.07 (1H, *s*, H(2)), 12.65 (1H, *s*, NH). <sup>13</sup>C NMR (CDCl<sub>3</sub>): δ = 14.4 (OCH<sub>2</sub>CH<sub>3</sub>), 17.3 (CH<sub>3</sub>), 60.8 (OCH<sub>2</sub>), 114.1 (C(3)), 116.6 (C(3')), 118.5 (C(8)), 123.9 (C(4a)), 126.6 (C(6)), 126.9 (C(5)), 135.3 (C(7)), 156.1 (C(8a)), 157.1 (C(4')), 158.4 (C(1')), 161.0 (CONH), 162.8 (COOCH<sub>2</sub>), 163.3 (C(2)), 176.5 (C(4)). *MS/EI m/z*: 359 (M+1, 64), 358 (M<sup>+</sup>, 98), 313 (37), 174 (73), 173 (93), 121 (100).

Method B: To a solution of chromone-2-carboxylic acid (1.1 mmol) in DMF (1.5 mL), POCl<sub>3</sub> (1 mmol) was added. The mixture was stirred at room temperature for 30 min, with the formation *in situ* of the corresponding acyl chloride. Then the aromatic amine or the heteroaromatic amine was added. The system was heated at 120 °C for 5 min in a microwave apparatus. Subsequently, the mixture was poured in a beaker and water was added. The formed solid was filtered and purified by recrystallization (CH<sub>2</sub>Cl<sub>2</sub>/n-Hexane) or flash chromatography (AcOEt/n-hexane).

*N*-(2-Methoxyphenyl)-4-oxo-4*H*-chromene-2-carboxamide (**19**): the synthetic procedure and structural elucidation data was described elsewhere.<sup>28</sup>

*N*-(3-Methoxyphenyl)-4-oxo-4*H*-chromene-2-carboxamide (**20**): the synthetic procedure and structural elucidation data was described elsewhere.<sup>28</sup>

*N*-(2,3-Dimethylphenyl)-4-oxo-4*H*-chromene-2-carboxamide (**23**): Yield: 68%. <sup>1</sup>H NMR (CDCl<sub>3</sub>): δ = 2.15 (3H, *s*, CH<sub>3</sub>), 2.32 (3H, *s*, CH<sub>3</sub>), 6.96 (1H, *s*, H(3)), 7.25-7.12 (3H, *m*, H(4'), H(5'), H(6')), 7.58 (1H, *ddd*, *J* = 1.08, 7.18, 8.07, H(6)), 7.83 (1H, *dd*, *J* = 0.58, 8.41, H(8)), 7.94 (1H, *ddd*, *J* = 1.70, 7.11, 8.68, H(7)), 8.10 (1H, *dd*, *J* = 1.41, 7.99, H(5)), 10.60 (1H, *s*, NH). <sup>13</sup>C NMR (CDCl<sub>3</sub>): δ = 14.2 (CH<sub>3</sub>), 20.0 (CH<sub>3</sub>), 110.8 (C(3)), 118.9 (C(8)), 123.6 (C(4a)), 124.4 (C(6')), 124.9 (C(6)), 125.4 (C(5')), 126.0 (C(5)), 128.2 (C(4')), 132.7 (C(2')), 134.6 (C(1')), 135.0 (C(7)), 137.0 (C(3')), 155.1 (C(8a)), 155.7 (C(2)), 157.9 (CONH), 177.2 (C(4)). *MS/EI m/z*: 293 (M<sup>+</sup>, 40), 292 (100), 264 (13), 120 (21).

*N*-(4-Methoxy-2-methylphenyl)-4-oxo-4*H*-chromene-2-carboxamide (**25**): Yield: 64%. <sup>1</sup>H NMR (CDCl<sub>3</sub>): δ = 2.35 (3H, *s*, CH<sub>3</sub>), 3.79 (3H, *s*, OCH<sub>3</sub>), 6.81-6.75 (2H, *m*, H(3'), H(5')), 7.22 (1H, *s*, H(3)), 7.47 (1H, *appt*, *J* = 8.0, 8.0, H(6)), 7.56 (1H, *d*, *J* = 8.1, H(8)), 7.72 (1H, *d*, *J* = 8.4, H(6')), 7.76 (1H, *ddd*, *J* = 1.7, 7.2, 8.7, H(7)), 8.23 (1H, *dd*, *J* = 8.0, 1.6, H(5)), 8.43 (1H, *s*, NH). <sup>13</sup>C

NMR (CDCl<sub>3</sub>): δ = 18.0 (CH<sub>3</sub>), 55.4 (OCH<sub>3</sub>), 111.8 (C(3)), 112.4 (C(6')), 116.2 (C(5')), 118.0 (C(8)), 124.3 (C(4a)), 125.0 (C(6)), 126.1 (C(3')), 126.1 (C(5)), 127.0 (C(1')), 132.2 (C(2')), 134.6 (C(7)), 154.8 (C(8a)), 155.1 (C(2)), 157.1 (C(4')), 157.8 (CONH), 178.0 (C(4)). *MS/EI m/z*: 310 (23), 309 (M<sup>+</sup>, 100), 195 (26), 136 (72).

Ethyl 4-methyl-2-(4-oxo-4*H*-chromene-3-carboxamido)thiazole-5-carboxylate (**32**): the synthetic procedure and structural elucidation data was described elsewhere.<sup>41</sup>

Method C: To a solution of chromone-3-carboxylic acid (500 mg, 2.6 mmol) in DMF (4 mL), POCl<sub>3</sub> (241 μL, 2.6 mmol) was added. The mixture was stirred at room temperature for 30 min, with the formation *in situ* of the corresponding acyl chloride. Then the heteroaromatic amine was added. After 1-5 hours, the mixture was diluted with dichloromethane (20 mL), washed with H<sub>2</sub>O (2X10 mL) and with saturated NaHCO<sub>3</sub> solution (2X10 mL). The organic phase was dried with Na<sub>2</sub>SO<sub>4</sub>, filtered, and concentrated under reduced pressure. The residue was purified by flash chromatography or crystallization.

*N*-(5-Methylthiazol-2-yl)-4-oxo-4*H*-chromene-3-carboxamide (**33**): yield: 15%. <sup>1</sup>H NMR (CDCl<sub>3</sub>): δ = 2.43 (3H, *d*, *J* = 1.2, CH<sub>3</sub>), 7.19 – 7.12 (1H, *m*, H(4')), 7.54 (1H, *ddd*, *J* = 1.0, 7.2, 8.1, H(6)), 7.59 (1H, *dd*, *J* = 0.6, 8.5, H(8)), 7.80 (1H, *ddd*, *J* = 1.7, 7.2, 8.7, H(7)), 8.35 (1H, *dd*, *J* = 1.5, 8.0, H(5)), 9.05 (1H, *s*, H(2)), 12.43 (1H, *s*, NH). <sup>13</sup>C NMR (CDCl<sub>3</sub>): δ = 11.7 (CH<sub>3</sub>), 114.6 (C(3)), 118.6 (C(8)), 124.1 (C(4a)), 126.7 (C(6)), 126.9 (C(5)), 128.4 (C(3')), 135.2 (C(7)), 135.4 (C(4')), 155.5 (C(1')), 156.2 (C(8a)), 160.3 (CONH), 163.0 (C(2)), 176.7 (C(4)). *MS/EI m/z*: 286 (M<sup>+</sup>, 91), 174 (30), 173 (100), 121 (61).

*N*-(4,5-Dimethylthiazol-2-yl)-4-oxo-4*H*-chromene-3-carboxamide (**34**): yield: 15%. <sup>1</sup>H NMR (CDCl<sub>3</sub>): δ = 2.28 (1H, *s*, CH<sub>3</sub>), 2.32 (1H, *s*, CH<sub>3</sub>), 7.54 (1H, *ddd*, *J* = 1.0, 7.2, 8.1, H(6)), 7.59 (1H, *dd*, *J* = 0.6, 8.5, H(8)), 7.79 (1H, *ddd*, *J* = 1.7, 7.2, 8.7, H(7)), 8.35 (1H, *dd*, *J* = 1.6, 8.0, H(5)), 9.04 (1H, *s*, H(2)), 12.37 (1H, *s*, NH). <sup>13</sup>C NMR (CDCl<sub>3</sub>): δ = 11.0 (CH<sub>3</sub>), 14.7 (CH<sub>3</sub>), 114.7 (C(3)), 118.6 (C(8)), 120.9 (C(3')), 124.1 (C(4a)), 126.7 (C(6)), 126.8 (C(5)), 135.2 (C(5)), 143.0 (C(4')), 152.9 (C(1')), 156.2 (C(8a)), 160.3 (CONH), 163.0 (C(2)), 176.7 (C(4)). *MS/EI m/z*: 302 (M+2), 300 (M<sup>+</sup>, 100), 199 (45), 139 (73).

#### Pharmacology

**CHO Membrane Preparation.** All methods involving membrane preparation for radioligand binding experiments followed the procedures as described earlier.<sup>32</sup> Membranes for radioligand binding were prepared from CHO cells stably transfected with the human adenosine receptor subtypes A<sub>1</sub>, A<sub>2A</sub>, and A<sub>3</sub> in a two-step procedure. In the first low-speed step (1,000g for 10 min at 4°C), the cell fragments and nuclei were removed. After that, the crude membrane fraction was sedimented from the supernatant at 100,000g for 30 min. The membrane pellet was then resuspended in the specific buffer used for the respective binding experiments, frozen in liquid nitrogen, and stored at -80°C. For the measurement of the

adenylyl cyclase activity in  $A_{2B}$  receptor expressing CHO cells, only one step of centrifugation was used in which the homogenate was sedimented for 30 min at 54,000g. The resulting crude membrane pellet was resuspended in 50 mM Tris/HCl, pH 7.4 and immediately used for the adenylyl cyclase assay.

#### Human Cloned $A_1$ , $A_{2A}$ , $A_3$ Adenosine Receptor Binding Assay.

All Binding of [ $^3$ H]CCPA to CHO cells transfected with the human recombinant  $A_1$  adenosine receptor was performed as previously described.<sup>32</sup> Competition experiments were performed for 3h at 25°C in 200  $\mu$ L of buffer containing 1 nM [ $^3$ H]CCPA, 0.2 U/mL adenosine deaminase, 20  $\mu$ g of membrane protein in 50 mM Tris/HCl, pH 7.4 and tested compound in different concentrations. Nonspecific binding was determined in the presence of 1 mM theophylline. Binding of [ $^3$ H]NECA to CHO cells transfected with the human recombinant  $A_{2A}$  adenosine receptors was performed following the conditions as that described for the  $A_1$  receptor binding.<sup>32</sup> In the competition experiments, samples containing a protein concentration of 50  $\mu$ g, 10 nM [ $^3$ H]NECA and tested compound in different concentrations were incubated for 3h at 25°C. Nonspecific binding was determined in the presence of 100  $\mu$ M R-PIA (R- $N^6$ -phenylisopropyladenosine). Binding of [ $^3$ H]HEMADO to CHO cells transfected with the human recombinant  $A_3$  adenosine receptors was carried out as previously described.<sup>32</sup> The competition experiments were performed for 3h at 25°C in buffer solution containing 1 nM [ $^3$ H]HEMADO, 20  $\mu$ g membrane protein in 50mM Tris-HCl, 1 mM ethylenediaminetetraacetate (EDTA), 10 mM  $MgCl_2$ , pH 8.25 and tested compound in different concentrations. Nonspecific binding was determined in the presence of 100  $\mu$ M R-PIA.

**Adenylyl Cyclase Activity.** Due to the lack of a suitable radioligand for  $hA_{2B}$  receptor in binding assay, the potency of antagonists at  $A_{2B}$  receptor (expressed on CHO cells) was determined in adenylyl cyclase experiments instead. The procedure was carried out as described previously with minor modifications.<sup>31, 32</sup> Membranes were incubated with about 150000 cpm of [ $\alpha$ - $^{32}$ P]ATP for 20 min in the incubation mixture as described, without EGTA and NaCl. For agonists, the  $EC_{50}$  values for the stimulation of adenylyl cyclase were calculated with the Hill equation. Hill coefficients in all experiments were near unity.  $IC_{50}$  values for concentration-dependent inhibition of NECA-stimulated adenylyl cyclase caused by antagonists were calculated accordingly. Dissociation constants ( $K_i$ ) for antagonist were then calculated from the Cheng and Prusoff equation.<sup>33</sup>

#### Molecular Modeling

A homology model of  $hA_3$  was constructed using MOE software.<sup>43</sup> Detailed description of the homology models are provided in previous publications of our research group.<sup>21</sup> The crystal structure of the  $hA_{2A}$  adenosine receptor (PDB: 3EML)<sup>35</sup> was used as a template in the modeling. Alignment between

both proteins was carried out considering highly conserved residues of the transmembrane helices. The same alignment described by Katritch *et al.* was followed.<sup>43</sup> The quality of the geometry in the protein homology models was assessed using the Protein Geometry module in MOE that takes into account Phi-Psi dihedral plots, bond lengths, bond angles, dihedrals, side chain rotamers and non-bonded contacts. The presence of conserved disulfide bridges between adenosine receptors was checked, such as the disulfide bridge in  $hA_3$  between Cys166 (EL2) and Cys83 (TM3). An optimization of the protein pocket using the Induce Fit Docking workflow was carried out.<sup>36</sup> This procedure included docking of high affinity ligands through Glide and protein active site optimization with Prime. Different  $hA_3$  models were tested, in a similar way as Katritch *et al.*,<sup>43</sup> according to their potential to discriminate ligands from decoys and  $hA_3$  high affinity compounds from other adenosine sub-types ligands. Areas under the ROC curves (AUROCs) were calculated showing results for some models greater than 0.80. The best  $hA_3$  models were selected to run molecular docking calculations.

#### Molecular Docking of Adenosine Receptors Ligands ( $hA_{2A}$ and $hA_3$ )

Molecular docking simulations were carried out using the Schrödinger package.<sup>36</sup> The database of chromone derivatives was pre-processed with LigPrep module. The structures were optimized and different tautomers and protonation states (pH=7.0 $\pm$ 2.0) were generated. Protein structures were also prepared with the Protein Preparation Wizard workflow.<sup>36</sup> This process includes different steps, i.e., assigned bond orders, added cap termini, optimized the hydrogen-bonding network and protonation states of some residues, among others. The molecular docking using the  $hA_{2A}$  crystallized structure (PDB code: 3EML)<sup>35</sup> and the homology model for the  $hA_3$  was carried out. No water molecules in the pocket of  $hA_3$  were included in the docking calculations. For the  $hA_{2A}$ , calculations without water and with water were performed. The compounds were docked with Glide module. Selection of the described binding modes was carried out taking into account the energetic parameter  $E_{model}$  and number of similar poses yielded by the calculations.

#### Acknowledgements

The authors would like to thank Fundação para a Ciência e Tecnologia (FCT) -Pest/C-QUI/UI0081/2013- and "Angeles Alvareño, Plan Galego de Investigación, Innovación e Crecemento 2011-2015 (I2C)" for the financial support. Thanks are due to Fundação para a Ciência e Tecnologia (FCT), Programa Operacional Potencial Humano (POPH) and Quadro de Referência Estratégica Nacional (QREN) for the post-doctoral and doctoral grants: A. Gaspar (SFRH/BPD/93331/2013), F. Cagide (SFRH/BPD/74491/2010) and J. Reis (SFRH/BD/96033/2013).

## Notes and references

- 1 J. F. Chen, H. K. Eltzschig and B. B. Fredholm, *Nat. Rev. Drug Discov.*, 2013, **12**, 265-286.
- 2 B. B. Fredholm, A. P. Ijzerman, K. A. Jacobson, J. Linden and C. E. Muller, *Pharmacol. Rev.*, 2011, **63**, 1-34.
- 3 S. Moro, Z. G. Gao, K. A. Jacobson and G. Spalluto, *Med. Res. Rev.* 2006, **26**, 131-159.
- 4 P. G. Baraldi, D. Preti, P. A., Borea and K. Varani, *J. Med. Chem.* 2012, **55**, 5676-5703.
- 5 C. E. Muller and K. A. Jacobson, *Biochim. Biophys. Acta* 2011, **1808**, 1290-1308.
- 6 J. Spychala, *Pharmacol. Ther.* 2000, **87**, 161-173.
- 7 S. Gessi, S. Merighi, V. Sacchetto, C. Simioni and P. A. Borea, *Biochim. Biophys. Acta* 2011, **1808**, 1400-1412.
- 8 P. A. Borea, K. Varani, F. Vincenzi, P. G. Baraldi, M. A. Tabrizi, S. Merighi and S. Gessi, *Pharmacol. Rev.* 2015, **67**, 74-102.
- 9 P. Fishman, S. Bar-Yehuda, B. T. Liang and K. A. Jacobson, *Drug Discov. Today* 2012, **17**, 359-366.
- 10 P. G. Baraldi, B. Cacciari, R. Romagnoli, S. Merighi, K. Varani, P. A. Borea and G. Spalluto, *Med. Res. Rev.* 2000, **20**, 103-128.
- 11 K. N. Klotz, N. Falgner, S. Kachler, C. Lambertucci, S. Vittori, R. Volpini and G. Cristalli, *Eur. J. Pharmacol.* 2007, **556**, 14-18.
- 12 R. Volpini, M. Buccioni, D. Dal Ben, C. Lambertucci, C. Lammi, G. Marucci, A. T. Ramadori, K. N. Klotz and G. Cristalli, *J. Med. Chem.* 2009, **52**, 7897-7900.
- 13 S. Taliani, C. La Motta, L. Mugnaini, F. Simorini, S. Salerno, A. M. Marini, F. Da Settimo, S. Cosconati, B. Cosimelli, G. Greco, V. Limongelli, L. Marinelli, E. Novellino, O. Ciampi, S. Daniele, M. L. Trincavelli and C. Martini, *J. Med. Chem.* 2010, **53**, 3954-3963.
- 14 S. Gessi, S. Merighi, K. Varani, E. Leung, S. Mac Lennan and P. A. Borea, *Pharmacol. Ther.* 2008, **117**, 123-140.
- 15 P. Fishman, K. A. Jacobson, A. Ochaion, S. Cohen and S. Bar-Yehuda, *Immunol. Endocr. Metab. Agents Med. Chem.* 2007, **7**, 298-303.
- 16 L. Madi, S. Bar-Yehuda, F. Barer, E. Ardon, A. Ochaion and P. Fishman, *J. Biol. Chem.* 2003, **278**, 42121-42130.
- 17 P. G. Baraldi, M. A. Tabrizi, A. Bovero, B. Avitabile, D. Preti, F. Frutterolo, R. Romagnoli, K. Varani and P. A. Borea, *Eur. J. Med. Chem.* 2003, **38**, 367-382.
- 18 H. Kim, J. W. Kang, S. Lee, W. J. Choi, L. S. Jeong, Y. Yang, J. T. Hong and D. Y. Yoon, *Anticancer Res.* 2010, **30**, 2823-2830.
- 19 P. Mlejnek, P. Dolezel and I. Frydrych, *J. Physiol. Biochem.* 2013, **69**, 405-417.
- 20 M. J. Matos, A. Gaspar, S. Kachler, K. N. Klotz, F. Borges, L. Santana and E. Uriarte, *J. Pharm. Pharmacol.* 2013, **65**, 30-34.
- 21 M. J. Matos, S. Vilar, S. Kachler, A. Fonseca, L. Santana, E. Uriarte, F. Borges, N. P. Tatonetti and K. N. Klotz, *ChemMedChem* 2014, **9**, 2245-2253.
- 22 X. Ji, N. Melman and K. A. Jacobson, *J. Med. Chem.* 1996, **39**, 781-788.
- 23 Y. Karton, J. Jiang, X. Ji, N. Melman, M. E. Olah, G. L. Stiles and K. A. Jacobson, *J. Med. Chem.* 1996, **39**, 2293-2301.
- 24 K. A. Jacobson, S. Moro, J. A. Manthey, P. L. West and X. D. Ji, *Adv. Exp. Med. Biol.* 2002, **505**, 163-171.
- 25 A. Gaspar, M. J. Matos, J. Garrido, E. Uriarte and F. Borges, *Chem. Rev.* 2014, **114**, 4960-4992.
- 26 A. Gaspar, J. Reis, S. Kachler, S. Paoletta, E. Uriarte, K. N. Klotz, S. Moro and F. Borges, *Biochem. Pharmacol.* 2012, **84**, 21-29.
- 27 A. Gaspar, A.; J. Reis, M. J. Matos, E. Uriarte and F. Borges, *Eur. J. Med. Chem.* 2012, **54**, 914-918.
- 28 A. Gaspar, F. Cagide, E. Quezada, J. Reis, E. Uriarte and F. Borges, *Magn. Reson. Chem.* 2013, **51**, 251-254.
- 29 J. Reis, A. Gaspar, F. Borges, L. R. Gomes and J. N. Low, *J. Mol. Struct.* 2014, **1056-1057**, 31-37.
- 30 F. Cagide, T. Silva, J. Reis, A. Gaspar, F. Borges, L. R. Gomes and J. N. Low, *Chem. Comm.* 2015, **51**, 2832-2835.
- 31 K. N. Klotz, G. Cristalli, M. Grifantini, S. Vittori and M. J. Lohse, *J. Biol. Chem.* 1985, **260**, 14659-14664.
- 32 K. N. Klotz, J. Hessling, J. Hegler, C. Owman, B. Kull, B. B. Fredholm and M. J. Lohse, *Naunyn. Schmiedebergs Arch. Pharmacol.* 1998, **357**, 1-9.
- 33 Y. Cheng and W. H. Prusoff, *Biochem. Pharmacol.* 1973, **22**, 3099-3108.
- 34 A. Delean, A. A. Hancock and R. J. Lefkowitz, *Mol. Pharm.* 1982, **21**, 5-16.
- 35 V. P. Jaakola, M. T. Griffith, M. A. Hanson, V. Cherezov, E. Y. Chien, J. R. Lane, A. P. Ijzerman and R. C. Stevens, *Science* 2008, **322**, 1211-1217.
- 36 Schrödinger suite 2014-3, Schrödinger, LLC, New York, USA, 2014. Available at: <http://www.schrodinger.com/> (Accessed: Nov 2014).
- 37 M. Congreve, S. P. Andrews, A. S. Dore, K. Hollenstein, E. Hurrell, C. J. Langmead, J. S. Mason, I. W. Ng, B. Tehan, A. Zhukov, M. Weir and F. H. Marshall, *J. Med. Chem.* 2012, **55**, 1898-1903.
- 38 V. P. Jaakola, J. R. Lane, J. Y. Lin, V. Katritch, A. P. Ijzerman and R. C. Stevens, *J. Biol. Chem.* 2010, **285**, 13032-13044.
- 39 F. Cagide, J. Reis, A. Gaspar and F. Borges, *Tetrahedron Lett.* 2011, **52**, 6446-6449.
- 40 A. Gaspar, J. Reis, A. Fonseca, N. Milhazes, D. Viña, E. Uriarte and F. Borges, *Bioorg. Med. Lett.* 2011, **21**, 707-709.
- 41 F. Cagide, F. Borges, L. R. Gomes and J. N. Low, *J. Mol. Struct.* 2015, **1089**, 206-215.
- 42 MOE, version 2011.10; Chemical Computing Group, Inc.: Available at: <http://www.chemcomp.com>. (Accessed: Jan 2012).
- 43 V. Katritch, I. Kufareva and R. Abagyan, *Neuropharmacology* 2011, **60**, 108-115.
- 44 M. F. Martins Borges, A. M. Neves Gaspar, J. M. Pinto de Jesus Garrido, N. J. Da Silva Pereira Milhazes, PT 103665, WO 2008/104925 A1, 2008.
- 45 A. Gaspar, T. Silva, M. Yáñez, D. Vina, F. Oralo, F. Ortuso, E. Uriarte, S. Alcaro, F. Borges *J. Med. Chem.* 2011, **54**, 5165-5173.